Taylor & Francis
Taylor & Francis Group

Biofouling
The Journal of Bioadhesion and Biofilm Research

ISSN: (Print) (Online) Journal homepage: www.tandfonline.com/journals/gbif20

Characterization of planktonic and biofilm cells from two filamentous cyanobacteria using a shotgun proteomic approach

Maria João Leal Romeu, Dany Domínguez-Pérez, Daniela Almeida, João Morais, Alexandre Campos, Vítor Vasconcelos & Filipe J. M. Mergulhão

To cite this article: Maria João Leal Romeu, Dany Domínguez-Pérez, Daniela Almeida, João Morais, Alexandre Campos, Vítor Vasconcelos & Filipe J. M. Mergulhão (2020) Characterization of planktonic and biofilm cells from two filamentous cyanobacteria using a shotgun proteomic approach, Biofouling, 36:6, 631-645, DOI: 10.1080/08927014.2020.1795141

To link to this article: https://doi.org/10.1080/08927014.2020.1795141

BIOFOULING
2020, VOL. 36, NO. 6, 631–645
https://doi.org/10.1080/08927014.2020.1795141

Taylor & Francis
Taylor & Francis Group

Characterization of planktonic and biofilm cells from two filamentous cyanobacteria using a shotgun proteomic approach

Maria João Leal Romeu[a], Dany Domínguez-Pérez[b], Daniela Almeida[b], João Morais[b], Alexandre Campos[b], Vítor Vasconcelos[b,c] and Filipe J. M. Mergulhão[a]

[a]LEPABE - Laboratory for Process Engineering, Environment, Biotechnology and Energy, Faculty of Engineering, University of Porto, Rua Dr. Roberto Frias, Porto, Portugal; [b]CIIMAR - Interdisciplinary Centre of Marine and Environmental Research, University of Porto, Terminal de Cruzeiros do Porto de Leixões, Matosinhos, Portugal; [c]Department of Biology, Faculty of Sciences, University of Porto, Rua do Campo Alegre, Porto, Portugal

ABSTRACT

Cyanobacteria promote marine biofouling with significant impacts. A qualitative proteomic analysis, by LC-MS/MS, of planktonic and biofilm cells from two cyanobacteria was performed. Biofilms were formed on glass and perspex at two relevant hydrodynamic conditions for marine environments (average shear rates of $4\,s^{-1}$ and $40\,s^{-1}$). For both strains and surfaces, biofilm development was higher at $4\,s^{-1}$. Biofilm development of *Nodosilinea* sp. LEGE 06145 was substantially higher than *Nodosilinea* sp. LEGE 06119, but no significant differences were found between surfaces. Overall, 377 and 301 different proteins were identified for *Nodosilinea* sp. LEGE 06145 and *Nodosilinea* sp. LEGE 06119. Differences in protein composition were more noticeable in biofilms formed under different hydrodynamic conditions than in those formed on different surfaces. Ribosomal and photosynthetic proteins were identified in most conditions. The characterization performed gives new insights into how shear rate and surface affect the planktonic to biofilm transition, from a structural and proteomics perspective.

ARTICLE HISTORY
Received 13 May 2020
Accepted 6 July 2020
Published online 26 July 2020

KEYWORDS
Marine biofouling; cyanobacterial biofilms; shotgun proteomics; LC-MS/MS; hydrodynamic conditions; real-time imaging; optical coherence tomography

Introduction

Marine biofouling causes several ecological problems and severe economic impacts on aquatic environments and marine industries (Carvalho 2018). Biofilm formation on submerged equipment containing optical and electrochemical sensors (which are used for on-site monitoring with continuous measuring) can affect readings and lead to incorrect measurements (Delauney et al. 2010). Cyanobacteria and diatoms are responsible for the initiation of biofilm formation by the production of large amounts of extracellular polymeric substances (EPS), and they also represent the major components of marine biofilms (Bharti et al. 2017). Additionally, these microfouler organisms can promote the adhesion of macrofouler organisms such as invertebrate larvae, mussels, seaweeds and barnacles (Mieszkin et al. 2013).

Physico-chemical factors related to the surface being colonized (Crawford et al. 2012) and flow velocity and shear rate (Allen et al. 2018) are some of the most critical parameters that affect biofilm composition, structure and development. Moreover, these factors can also impact EPS production, energy metabolism and induce molecular changes in biofilms (Moreira et al. 2015). The development of novel antifouling strategies for marine applications is of paramount importance (Telegdi et al. 2016). Therefore, molecular studies capable of identifying the agents and pathways affecting the settlement of biofouling organisms are necessary to obtain new targets and develop more effective biofilm mitigation strategies.

Omics approaches such as genomics, transcriptomics, proteomics and metabolomics have been widely used to characterize bacterial virulence factors (Alexova et al. 2011; Babele et al. 2019) and provide new information about biofilm development and regulation (Leary et al. 2014; Parnasa et al. 2016). Specifically, proteomic studies have also been used to understand the molecular mechanisms involved in important cellular processes such as cell division, metabolism, transport, stress response and motility in these microbial communities (Parnasa et al. 2016;

CONTACT Filipe J. M. Mergulhão filipem@fe.up.pt
Supplemental data for this article can be accessed at https://doi.org/10.1080/08927014.2020.1795141.

Wang et al. 2020). Furthermore, proteomic analysis allows the study of interspecies interactions on biofilms (Herschend et al. 2017) and how biofilm development is affected by physiological and environmental factors (Chen et al. 2019). In a stressful condition, the long-term adaptation is governed by mechanisms of cellular regulation as the synthesis and/or modified expression of proteins. The identification of these proteins using high throughput proteomic tools has provided new insights into the cellular response to a defined stress condition and also regarding the cell signaling and stress response pathways that are activated under different conditions (Muthusamy et al. 2017; Battchikova et al. 2018). Since modifications in the proteome are associated with physiological and metabolic rearrangements at the genotype level during stress adaptation and tolerance, qualitative proteomic studies lead to the identification and characterization of these stress-responsive proteins (Babele et al. 2019). Therefore, qualitative proteomic experiments can provide a general picture of the physiological state of a given organism through the identification of proteins which are translated under different conditions.

The isolation and purification of stable and high-quality proteins is the most challenging task in cyanobacterial proteomic experiments (Pandhal et al. 2009), since cyanobacteria contain several proteases, oxidative enzymes, phycobiliproteins and other pigments which hinder the effective extraction, purification and recovery of less abundant proteins (Ow et al. 2011). In this context, novel extraction protocols have been developed and were a major step for today's high throughput proteomic workflows (Anderson et al. 2006). The development of high-resolution liquid chromatography (LC) and more advanced tandem mass spectrometry (MS/MS) enabled the development of shotgun proteomics (Babele et al. 2019). Since proteomes are directly digested and analyzed *in situ* by a combination of liquid chromatographic separation and analysis using high-speed tandem mass spectrometry, shotgun proteomics opened up opportunities to perform fast and reliable identification of cyanobacterial proteins (Anderson et al. 2006). Furthermore, LC–MS/MS data acquisition is nearly fully automated, which enables analysis in a high throughput mode leading to low variations, thus, improving the confidence of the results.

Although several studies investigated the proteome of planktonic and sessile forms, only a few address marine biofilms (Leary et al. 2014). The data available on cyanobacteria are sparse (Babele et al. 2019) and focus on well-studied model cyanobacteria, such as the unicellular cyanobacterium *Synechocystis* sp. PCC 6803 (Jahn et al. 2018). Moreover, the small number of proteomic studies performed on filamentous cyanobacteria is rather old and restricted to the cyanobacterial genera *Nostoc*, *Anabaena* and *Spirulina* (Anderson et al. 2006; Kurdrid et al. 2011).

The main aim of this study was to perform a qualitative proteomic analysis on filamentous cyanobacteria under planktonic and different conditions of biofilm development. To the best of the authors' knowledge, there are no proteomic studies evaluating the impact of different surfaces and different hydrodynamic conditions on cyanobacterial biofilm behavior. Since no proteomic analysis of the genus *Nodosilinea* is available, this represents the first work that investigated the proteome obtained from different conditions of biofilm development of this ubiquitous cyanobacterial genus. Cyanobacterial strains from the genus *Nodosilinea* are present in dissimilar geographies, including different continents (Europe, Antarctica, Asia and America), and specimens can also be found in different ecologies, such as brackish water, freshwater, marine and even terrestrial environments (Heidari et al. 2018; Ramos et al. 2018; Vázquez-Martínez et al. 2018; Radzi et al. 2019). This cosmopolitan distribution highlights the importance of studying biofilm formation by these organisms. Moreover, the relevance of studying these filamentous cyanobacterial strains is even more critical given the biofouling potential of these organisms. Indeed, some studies showed the high biofouling potential of the genus *Nodosilinea* on different surfaces. Additionally, cyanobacterial strains from this genus were recovered from biofilms on a house wall (Perkerson Iii et al. 2011), from a benthic mat in a thermal spring with very high natural radioactivity (Heidari et al. 2018) and even from mats collected in Antarctica (Radzi et al. 2019). *Nodosilinea* strains were also found on subaerial biofilms, which develop on mineral surfaces and on archaeological stone monuments experiencing extended periods of heat, insolation and dehydration (Vázquez-Martínez et al. 2018). These biofilms have been widely studied due to their impact on deterioration of cultural heritage.

Materials and methods

Organism and inocula preparation

Two cyanobacterial strains were used in this study, and both were obtained from the Blue Biotechnology and Ecotoxicology Culture Collection (LEGE-CC)

located at CIIMAR, Portugal (Ramos et al. 2018). *Nodosilinea* sp. LEGE 06145 was isolated from a sample scraped from a wave-exposed rock in a tide puddle collected at Moledo beach, Portugal (41.84963 N 8.866717 W). *Nodosilinea* sp. LEGE 06119 was isolated from a seawater sample collected in the surf zone at Burgau beach, Portugal (37.07156 N 8.774722 W) (Ramos et al. 2018). Cells from an initial 50 ml culture were grown for 30 days in 750 ml of Z8 medium (Kotai 1972) supplemented with 25 g l^{-1} of synthetic sea salts (Tropic Marin) and vitamin B_{12} (Sigma Aldrich, Merck, St Louis, MO, USA). Cultures were performed under 14 h light (10–30 µmol photons m^{-2} s^{-1})/10 h dark cycles, at 25 °C.

Biofilm formation

Biofilm formation was assessed on agitated 12-well microtiter plates (VWR International, Carnaxide, Portugal), since this platform was shown to mimic the hydrodynamic conditions found in marine environments (Romeu et al. 2019). In order to assess the effect of the surface on protein expression, biofilms were developed on glass (Vidraria Lousada, Lda, Portugal) and perspex (Neves & Neves, Lda, Portugal) coupons (1 cm^2). These represent commonly submerged artificial surfaces found on different equipment in aquatic and marine environments (Taylor 1996; King et al. 2006). Moreover, these surfaces present different hydrophobicity (perspex is relatively hydrophobic compared with glass) (Romeu et al. 2019). Surface preparation was performed as described in Romeu et al. (2019). All coupons were aseptically pre-weighed. Transparent double-sided adhesive tape was used to fix the coupons and once the tape was placed in the wells, all coupons and the plates were subjected to UV sterilization for 30 min, after which the sterile coupons were fixed. Since chlorophyll *a* concentration is commonly used as biomass indicator in aquatic environments, prior to inoculation each cyanobacterial suspension was adjusted to a chlorophyll *a* concentration of 1.5 µg ml^{-1}. Briefly, 2 ml of each suspension were incubated for 24 h at 4 °C in the dark for a maximal chlorophyll *a* extraction. The samples were then centrifuged at 3,202 *g*, for 5 min at room temperature, and the supernatant was transferred to a glass cuvette. The absorbance at 750 nm (turbidity), 665 nm (chlorophyll *a*) and 652 nm (chlorophyll *b*) was determined using a V-1200 spectrophotometer (VWR International China Co., Ltd, Shanghai, China). The chlorophyll *a* concentration (µg cm^{-2}) was calculated by the following Equation (1) (Porra et al. 1989):

$$\mathrm{Chl}a\left(\mu g\ ml^{-1}\right) = 16.29 \times A^{665} - 8.54 \times A^{652} \quad (1)$$

These measurements were performed in triplicate and the dilutions were performed using Z8 medium supplemented with 25 g l^{-1} of synthetic sea salts and vitamin B_{12}. After cyanobacterial suspension adjustment, planktonic samples for proteomic analysis were collected and kept at −80 °C.

A volume of 3 ml of adjusted cyanobacterial suspension in Z8 medium (prepared as described above) supplemented with nutritional factors, which support the growth and cyanobacteria maintenance (Kotai 1972), was inoculated in each well. In order to assess the hydrodynamic effect on protein expression, cyanobacterial biofilm formation at different shear rates was tested. In order to attain the shear rate values that can mimic aquatic environments, such as those found on a ship hull in a harbor and in partially submerged or even moored equipment and devices (as underwater cameras, flotation spheres, sensors and even transparent hulls of boats or their windows), microtiter plates were incubated at 25 °C in an orbital shaker with a 25 mm orbital radius (Agitorb 200ICP, Norconcessus, Portugal) at 185 rpm (achieving the average shear rate of 40 s^{-1}, Romeu et al. 2019). Moreover, since lower fluid velocities can promote marine biofouling (Flemming et al. 2009), biofilm development was also assessed at lower shear rate conditions (average shear rate of 4 s^{-1}, achieved at 40 rpm). Biofilm development was followed for seven weeks (49 days) since it is accepted that a two-month interval for maintenance is the minimum duration for economically viable underwater monitoring systems, as previously reported (Romeu et al. 2019). During this incubation time, the medium was replaced twice a week. In order to mimic real light exposure periods, a photoperiod of 14 h light (8–10 µmol photons m^{-2} s^{-1})/10 h dark cycles) was applied.

Biofilm analysis

Sampling was performed every seven days and at each sampling day, three coupons for each surface and hydrodynamic condition were analyzed for both cyanobacteria. The culture medium was carefully removed and the wells were filled with 3 ml of sterile sodium chloride solution (8.5 g l^{-1}) to evaluate the cyanobacterial biofilm structure and thickness by

optical coherence tomography (OCT). In order to complement the characterization of cyanobacterial biofilms, the determination of their wet weight and chlorophyll *a* content was performed.

Optical coherence tomography

Images from cyanobacterial biofilms developed on both surfaces and under the different hydrodynamic conditions were captured as reported in Romeu et al. (2019). Briefly, the captured volume was $\sim 4 \times 4 \times 3\,mm^3$ ($509 \times 313 \times 1{,}024$ pixels^3) and since biofilms are mainly composed (90%) of water (Bakke et al. 2001), the refractive index was set to 1.40. For each coupon, 2-D imaging was performed with a minimum of three fields of view, to ensure the accuracy and reliability of the results obtained. Image analysis was performed using a routine developed in the Image Processing Toolbox from MATLAB 8.0 and Statistics Toolbox 8.1 (The MathWorks, Inc., Natick, MA, USA). The processing steps include image denoising, detection of the surface layer/biofilm bottom and segmentation of the biofilm structure by the upper contour line of the biofilm. The acquired image is denoised using Haar wavelets (Mayer et al. 2012). The method used for the detection of the biofilm bottom consists of edge detection, using the Canny edge filter (Canny 1986) and straight-line detection, using the Hough line transform (Duda and Hart 1972). The highest peak in Hough space corresponds to the surface layer and biofilm bottom. For the segmentation of the biofilm structure, a Sobel operator is applied, and the result is thresholded. Then, the resulting binary image is dilated, using a vertical structuring element and a horizontal structuring element and the holes inside the biofilm are filled in. Finally, the contours of the resulting binary image are smoothed, by eroding the image with a diamond structuring element. In this way, a binary "mask" that covers the biofilm region is obtained. The biofilm is delimited by the upper boundary of this "mask" and by the surface layer/biofilm bottom. The mean of biofilm thickness was calculated based in the distance between the biofilm bottom and the upper contour line according the following Equation (2):

$$\overline{L}_F = \frac{1}{N} \sum_{i=1}^{N} L_{F,i} \tag{2}$$

where $L_{F,i}$ is a local biofilm thickness measurements at location i and N equals the number of thickness measurements and $\overline{L}_F$ is the mean biofilm thickness.

Wet weight determination and chlorophyll *a* quantification

The determination of the wet weight and chlorophyll *a* content of cyanobacterial biofilms was performed as reported in Romeu et al. (2019). Briefly, to determine the wet weight, coupons were detached from the wells and weighed. Biofilm wet weight was obtained as the difference from the initial coupon weight (determined prior to inoculation). Afterward, cyanobacterial cells were detached from the coupons by immersing each coupon in 2 ml of 8.5 g l^{-1} sodium chloride solution and vortexing, and the suspensions were incubated for 24 h at 4 °C in the dark for a maximal chlorophyll *a* extraction, as previously described through Equation 1.

Proteomics analysis

Protein extraction and sample preparation

Biomass of 40 biofilm samples comprising four replicates from each biofilm condition of *Nodosilinea* sp. LEGE 06145 and *Nodosilinea* sp. LEGE 06119 and four samples consisting of two replicates from planktonic samples of both the cyanobacterial strains were kept at −80 °C until protein extraction. Biomass for biofilm samples was obtained as previously described. Briefly, cyanobacterial biofilms were detached from the coupons by immersing each coupon in 2 ml of 8.5 g l^{-1} sodium chloride solution and vortexing. The total protein extraction was performed into sodium dithionite (SDT) buffer (2% SDS, 100 mM Tris/HCl pH 7.6, 0.1 M DTT) + protease inhibitors (PIs, Roche, 11697498001), as a variant of the method carried out by Campos et al. (2016). Briefly, the biomass from each replicate was weighed and a proper volume of SDT buffer was added to the samples (0.5 g ml^{-1} SDT), sonicated 5×4 s and 23 kHz − 105 µm (amplitude) and incubated at room temperature overnight. Afterward, samples were sonicated 5×4 s and 23 kHz − 105 µm (amplitude), heated for 3 min at 95 °C and subsequently centrifuged at 16,000 *g* for 20 min. Finally, the supernatant was collected, and total protein concentration was measured indirectly by optical density (OD) at 280 nm using a microplate reader (PowerWave; Biotek, VT, USA). Samples containing the extracted protein were stored for 24 h at −20 °C.

The extracted proteins were processed using the Filter Aided Sample Preparation (FASP) protocol described by Wiśniewski et al. (2009). In summary, this approach comprised the alkylation and digestion of 30 µg of the extracted proteins with trypsin (recombinant, proteomics grade, Roche, Basel,

Switzerland) at an enzyme to protein ratio of 1:100 (w/w) for 16 h at 37 °C using centrifugal filter units with a nominal molecular weight limit (NMWL) of 30 kDa (MRCPRT030, Millipore, Billerica, MA, USA). Through centrifugal filtration, peptides were recovered and acidified with trifluoracetic acid (TFA) (10% v v^{-1}). Samples were desalted and concentrated by reversed-phase extractions (C18 Tips, 100 µl, Thermo Scientific, Bremen, Germany, 87784) with acetonitrile (ACN) (50% v v^{-1}) and TFA (0.1% v v^{-1}) for peptide elution. Before LC-MS/MS analysis, samples were dried in the speed-vac and resuspended in formic acid (FA) (0.1% v v^{-1}) to a final concentration of 0.04–0.06 µg $µl^{-1}$.

LC-MS/MS analysis

FASP protein digests were processed using a nano LC-MS/MS, composed by an Ultimate 3000 liquid chromatography system coupled to a Q-Exactive Hybrid Quadrupole – Orbitrap mass spectrometer (Thermo Scientific). Samples were loaded onto a trapping cartridge (Acclaim PepMap C18 100A˚, 5 mm × 300 µm i.d., 160454, Thermo Scientific) in a mobile phase of 2% ACN, 0.1% FA at 10 µl min^{-1}. After 3 min loading, the trap column was switched in-line to a 15 cm by 75 µm inner diameter EASY-Spray column (ES800, PepMap RSLC, C18, 3 µm, Thermo Scientific) at 300 ml min^{-1}. Separation was generated by mixing A: 0.1% FA and B: 80% ACN, with the following gradient: 5 min (2.5% B to 10% B), 60 min (10% B to 35% B), 5 min (35% B to 99% B) and 5 min (hold 99% B). Subsequently, the column was equilibrated with 2.5% B for 12 min. Data acquisition was controlled by Xcalibur 4.0 and Tune 2.8 software (Thermo Scientific). The mass spectrometer was operated in data-dependent (dd) positive acquisition mode alternating between a full scan (m/z 380–1,580) and subsequent HCD MS/MS of the 10 most intense peaks from full scan (normalized collision energy of 27%). ESI spray voltage was 1.9 kV and capillary temperature was 275 °C. Global settings: use lock masses best (m/z 445.12003), lock mass injection Full MS, chrom. peak width (FWHM) 15 s. Full scan settings: 70k resolution (m/z 200), AGC target 3e6, maximum injection time 50 ms. dd settings: minimum AGC target 8e3, intensity threshold 7.3e4, charge exclusion: unassigned, 1, 8, >8, peptide match preferred, exclude isotopes on, dynamic exclusion 20 s. MS2 settings: microscans 1, resolution 35k (m/z 200), AGC target 2e5, maximum injection time 110 ms, isolation window 2.0 m/z, isolation offset 0.0 m/z, spectrum data type profile.

Protein identification

The raw data were analyzed and processed using the Proteome Discoverer 2.2.0.388 software (Thermo Scientific) and searched against the UniProt database for Bacteria taxonomic selection (2018_07 release). The Sequest HT search engine was used for protein identification. The ion mass tolerance was 10 ppm for precursor ions and 0.02 Da for-fragment ions. The maximum allowed missing cleavage sites was set to 2. Cysteine carbamidomethylation was defined as a constant modification. Methionine oxidation and protein N-terminus acetylation were defined as variable modifications. Peptide confidence was set to high. The processing node Percolator was enabled with the following settings: maximum delta Cn 0.05; decoy database search target FDR 1%, validation was based on q-value.

Protein distribution among different conditions of biofilm development

The distribution of protein identified among replicates and among the different conditions was analyzed by Venn diagram using an online free tool, available at the webserver of the Bioinformatics and Evolutionary Genomics Center (BEG/Van de Peer Lab site), Ghent University, Belgium, http://bioinformatics.psb.ugent.be/webtools/Venn/. For comparison purposes, the identified proteins from all replicates of each treatment were merged into a single file and duplicates removed. Finally, the corresponding distribution of unique and shared proteins among different conditions were reported.

Statistical analysis

All experiments were performed in triplicate. Data analysis was performed using the statistical program GraphPad Prism® for Windows, version 6.01 (GraphPad Software, Inc., San Diego, CA, USA) and results were compared using unpaired *t*-tests with a confidence level of 95% (**; $p < 0.05$) and 90% (*; $p < 0.1$).

Results and discussion

Biofilm development analysis

Monitoring of cyanobacterial biofilm development was done for 49 days (progress of wet weight,

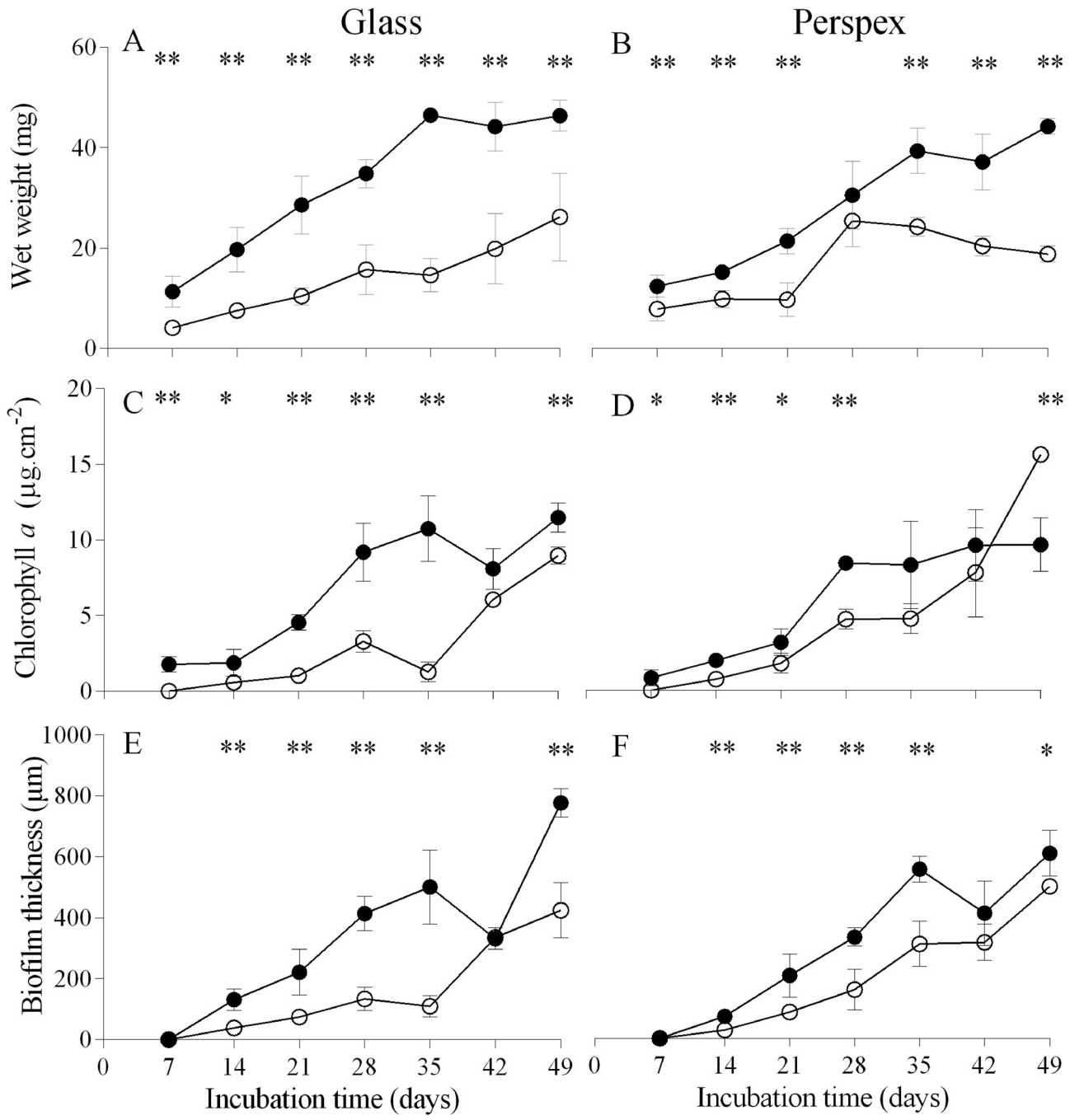

Figure 1. Evaluation of *Nodosilinea* sp. LEGE 06145 biofilm development. The parameters analyzed refer to wet weight (A, B), chlorophyll *a* (C, D) and biofilm thickness (E, F). Biofilms were formed in glass (A, C, E) or perspex (B, D, F), at two average shear rates, 4 s^{-1} (closed circles) and 40 s^{-1} (open circles) for 49 days. SDs from two biological assays with three replicates each are represented. Symbols * and ** indicate statistically different values for $p < 0.1$ and $p < 0.05$ (respectively) at each incubation time.

chlorophyll *a* and biofilm thickness), as shown in Figures 1 and 2. For both cyanobacterial strains and both surfaces, biofilm development was higher at the lowest shear rate. Compared with the values obtained at higher shear rate (40 s^{-1}), the biofilm mass obtained on a glass surface under lower shear conditions (4 s^{-1}) was on average 63.9% and 48% higher for *Nodosilinea* sp. LEGE 06145 (Figure 1a) and *Nodosilinea* sp. LEGE 06119 (Figure 2a), respectively. Likewise, on perspex, the biofilm wet weight was on average 40.6% higher for *Nodosilinea* sp. LEGE 06145 (Figure 1b) and 29.6% for *Nodosilinea* sp. LEGE 06119 (Figure 2b). The chlorophyll *a* content at 4 s^{-1} and on glass was, on average 64.6% and 98.8% higher for *Nodosilinea* sp. LEGE 06145 (Figure 1c) and *Nodosilinea* sp. LEGE 06119 (Figure 2c), respectively, whereas on perspex it was, on average, 35.7% higher for *Nodosilinea* sp. LEGE 06145 (Figure 1d) and

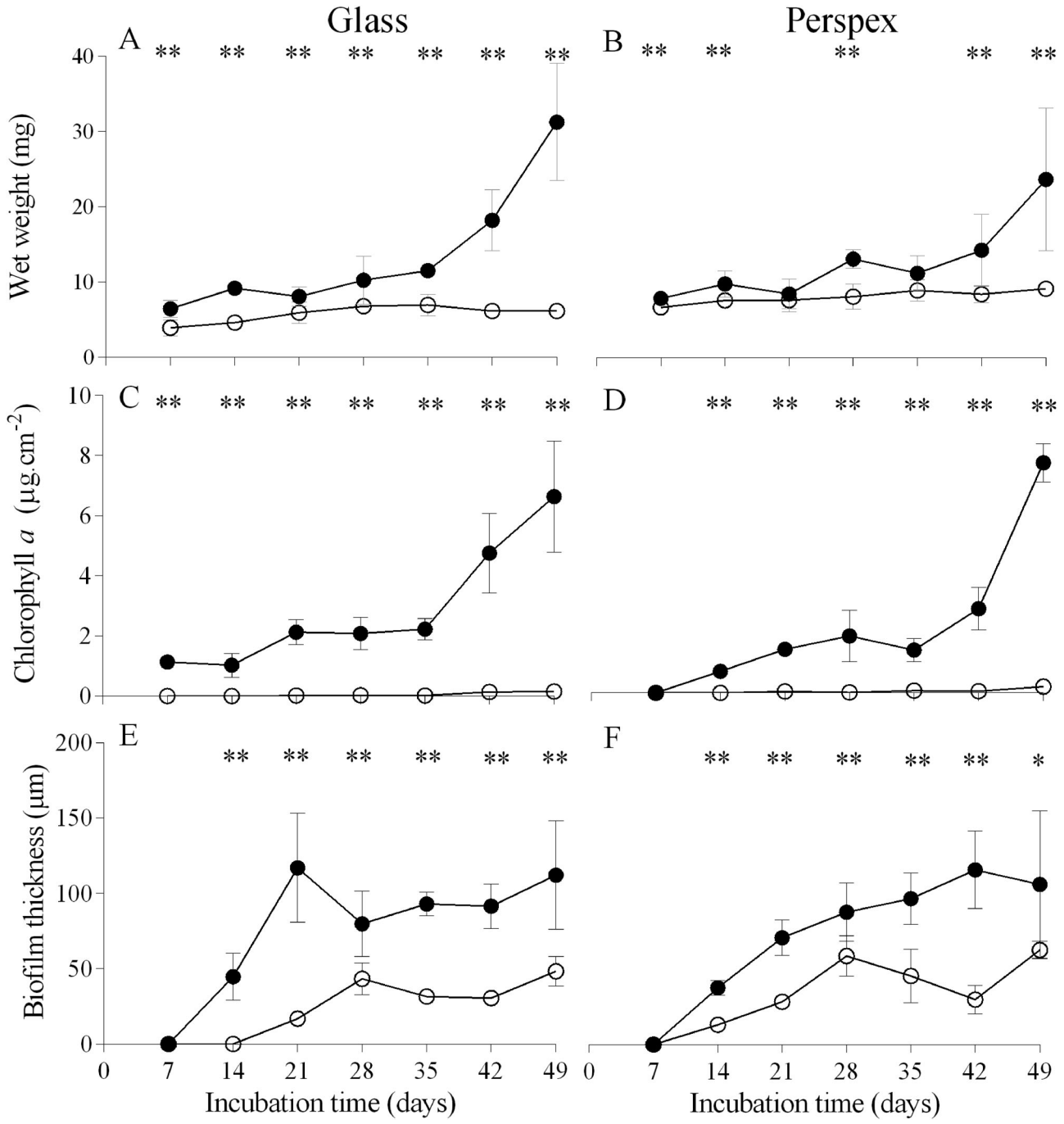

Figure 2. Evaluation of *Nodosilinea* sp. LEGE 06119 biofilm development. The parameters analyzed refer to wet weight (A, B), chlorophyll *a* (C, D) and biofilm thickness (E, F). Biofilms were formed in glass (A, C, E) or perspex (B, D, F), at two average shear rates, 4 s^{-1} (closed circles) and 40 s^{-1} (open circles) for 49 days. SDs from two biological assays with three replicates each are represented. Symbols * and ** indicate statistically different values for $p < 0.1$ and $p < 0.05$ (respectively) at each incubation time.

97.4% for *Nodosilinea* sp. LEGE 06119 (Figure 2d) compared with higher shear conditions. Since a correlation between chlorophyll *a* production and biofilm wet weight was observed (Supplementary material, SM1), chlorophyll *a* content monitorization was demonstrated to be a useful tool to follow cyanobacterial biofilm growth, as previously reported (Romeu et al. 2019).

Although some differences in biofilm development at different shear conditions were noticed in the early stages, major differences were found in the maturation phase of biofilm development (on general from day 28 and mainly in wet weight quantification), which corroborates previous results obtained with different cyanobacterial strains (Romeu et al. 2019). The increased shear rate during biofilm development may

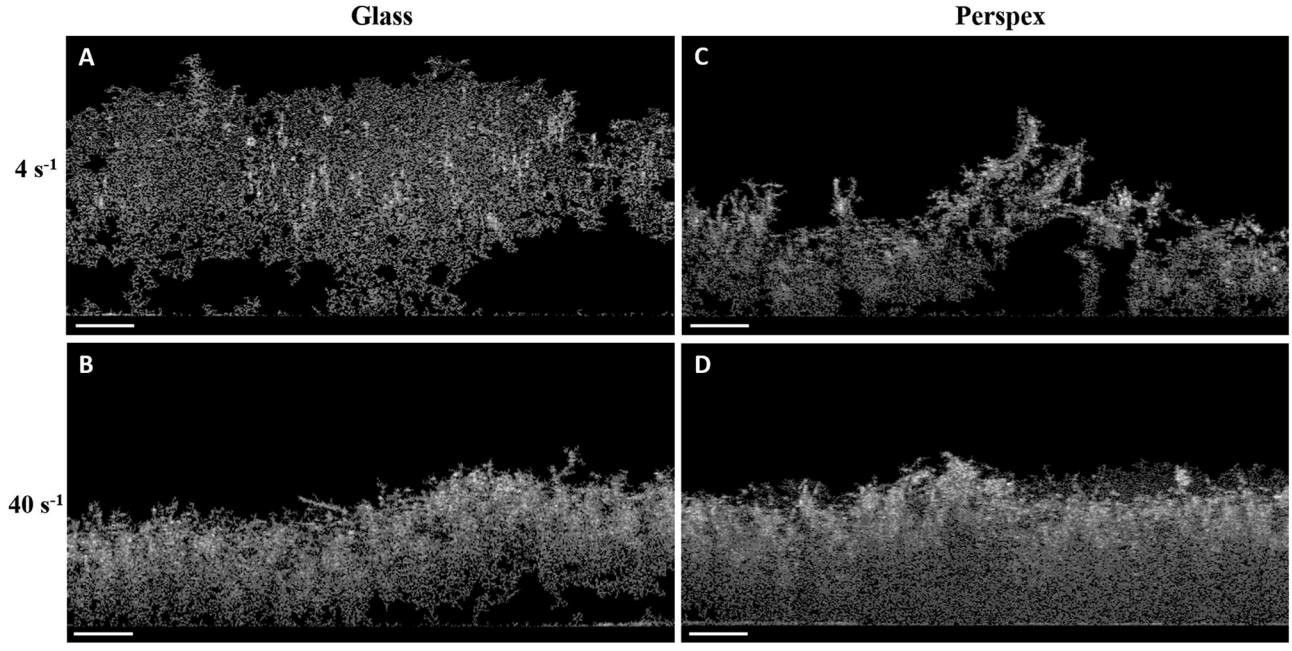

Figure 3. 2-D cross-sectional OCT images of *Nodosilinea* sp. LEGE 06145 biofilms formed after 49 days on glass and perspex at two different shear rates, 4 s^{-1} (A, C) and 40 s^{-1} (B, D). Scale bar = 200 µm.

promote sloughing events and erosion, affecting biofilm cohesion. Moreover, this difference in biofilm development between the two hydrodynamic conditions was more noticeable for *Nodosilinea* sp. LEGE 06119 (Figure 2a–d).

The biofilm thickness obtained on the glass surface under lower shear conditions was on average 54.5% and 64.2% higher for *Nodosilinea* sp. LEGE 06145 (Figure 1e) and *Nodosilinea* sp. LEGE 06119 (Figure 2e), respectively, when compared with those obtained at 40 s^{-1}. On perspex, the biofilm thickness was, on average 42.9% higher for *Nodosilinea* sp. LEGE 06145 (Figure 1f) and 54.3% for *Nodosilinea* sp. LEGE 06119 (Figure 2f). The highest value of biofilm thickness was observed at 4 s^{-1} on glass for *Nodosilinea* sp. LEGE 06145 (∼ 800 µm; Figure 1e, 49 days). Values of biofilm thickness obtained for *Nodosilinea* sp. LEGE 06119 were significantly lower, achieving a maximum of 120 µm at 4 s^{-1} on glass (Figure 2e). Indeed, all parameters analyzed showed that biofilm development by *Nodosilinea* sp. LEGE 06145 was substantially higher than by *Nodosilinea* sp. LEGE 06119 (Supplementary material, SM2).

Despite the different properties of glass and perspex, the latter of which is the most hydrophobic surface (Romeu et al. 2019), similar values of wet weight, chlorophyll *a* content and biofilm thickness were obtained for the biofilms formed on different surfaces at the same hydrodynamic conditions (Supplementary material, SM3). These findings, which show that the effect of surface hydrophobicity was less important than the hydrodynamic effect on cyanobacterial biofilm development, had previously been shown for other cyanobacterial strains (Romeu et al. 2019; Faria et al. 2020).

Figures 3 and 4 show representative 2-D cross-sectional images of *Nodosilinea* sp. LEGE 06145 and *Nodosilinea* sp. LEGE 06119, respectively, obtained from OCT at the end of the experiment (49 days). From these OCT images, the difference in biofilm development between the cyanobacterial strains is clear. Again, the differences in biofilm structure between hydrodynamic conditions were also more noticeable than between the two surfaces. Despite the lower biofilm biomass obtained at a higher shear rate (40 s^{-1}) for *Nodosilinea* sp. LEGE 06119 (Figure 4b, d), it is possible to observe that cyanobacterial biofilms obtained at 4 s^{-1} were less homogeneous in their structure, presenting three-dimensional streamers on the biofilm surface. The appearance of these structures was previously reported for other cyanobacterial biofilm formed under different hydrodynamic conditions (Romeu et al. 2019). Instead, biofilms formed under the higher shear rate presented a more compact structure. While a compacted structure may be relevant in biofilms formed under higher shear conditions to increase the biofilm cohesion and avoid biofilm sloughing and erosion, a lower degree of compaction in biofilms formed under lower shear rates is an appropriate adaptation to improve the mass transfer to the inner layers of the biofilm (Teodósio et al. 2011).

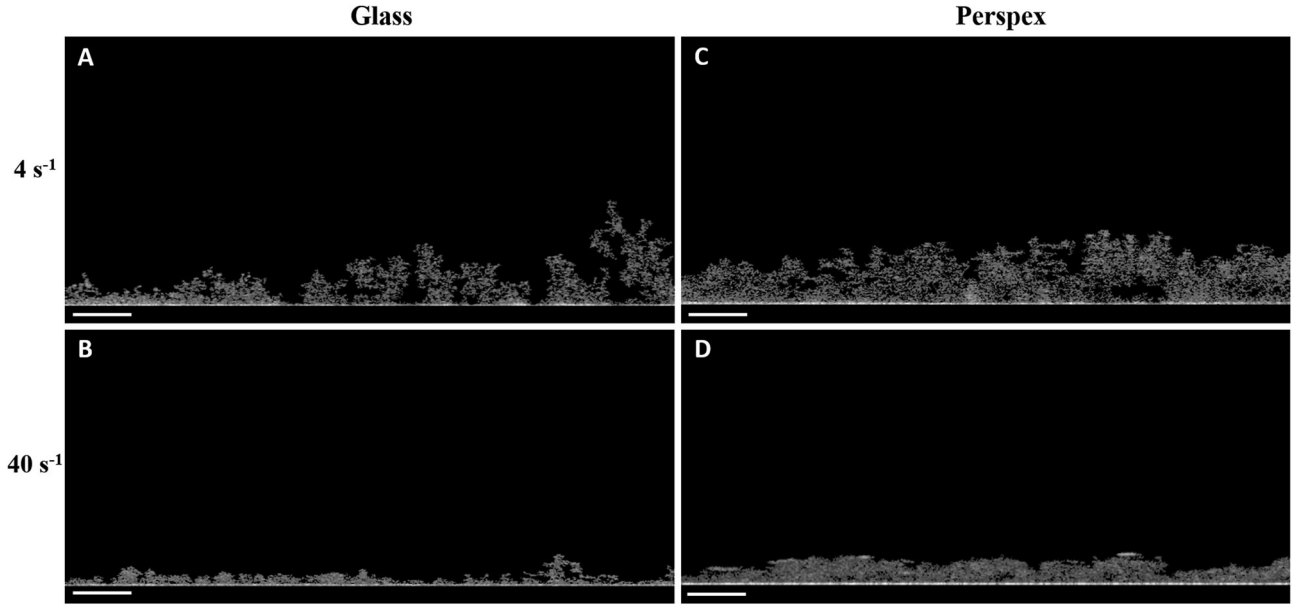

Figure 4. 2-D cross-sectional OCT images of *Nodosilinea* sp. LEGE 06119 biofilms formed after 49 days on glass and Perspex at two different shear rates, 4 s^{-1} (A, C) and 40 s^{-1} (B, D). Scale bar = 200 µm.

Proteomic analysis

A qualitative proteomic analysis by LC-MS/MS was performed, and the number and the distribution of proteins found for both cyanobacterial strains in different conditions is shown in Figure 5. The number of cyanobacterial proteins identified from all planktonic and biofilm samples is available in Supplementary material, SM4. A total of 377 and 301 different proteins were identified for *Nodosilinea* sp. LEGE 06145 and *Nodosilinea* sp. LEGE 06119, respectively, of which 108 were found in both cyanobacterial strains (Figure 5a). Among the 16 common proteins identified in the cyanobacterial planktonic samples (Figure 5b), none is exclusive to the planktonic form because they were identified in an additional biofilm condition. A previous quantitative proteomic study performed on the marine bacterium *Pseudoalteromonas lipolytica* TC8 also aimed at highlighting specific metabolic shifts between planktonic and biofilm cultures. This study showed that 90% of proteins were present in the proteomes of both planktonic and biofilm samples (Favre et al. 2018). Moreover, the percentage of proteins found in the four different biofilm conditions and which were identified in both cyanobacterial strains was similar and below 22%. Amongst the four possibilities tested for biofilm development, biofilms that were formed on perspex and at 40 s^{-1} showed a higher percentage of common proteins between the two cyanobacterial strains (21.1%, Figure 5f). Conversely, biofilms that were formed on perspex but at 4 s^{-1} showed a lower number of common proteins between the two cyanobacterial strains (7.8%, Figure 5d). A broad diversity in the protein expression profiles of each strain was observed. Similarly, substantial differences in protein expression among cyanobacterial strains at the same conditions were also observed in a study of *Microcystis aeruginosa* (Alexova et al. 2011) and only 29–43% of the identified proteins were found to be expressed in all six strains analyzed in this study. Moreover, a study performed with the marine cyanobacterium *Prochlorococcus* spp. showed that the elemental composition of their proteomes was strongly influenced by their site of isolation and the nutritional availability at that site (Lv et al. 2008). Since *Nodosilinea* sp. LEGE 06145 was isolated from a sample scraped from a wave-exposed rock in a tide puddle collected at Moledo beach and *Nodosilinea* sp. LEGE 06119 was isolated from a seawater sample collected in the surf zone collected at Burgau beach, the observed proteome diversity supports the view that strains should be considered as ecotypes adapted to survival in a particular environmental niche (Otsuka et al. 2001). For the same cyanobacterial strain, a higher number of proteins was identified on glass rather than on perspex, and comparing the two hydrodynamic conditions, a higher number of proteins was obtained at 4 s^{-1} for both cyanobacteria (Figure 5C–F). This lower shear condition corresponds to the scenario in which a higher amount of biofilm formation was observed (Figures 1–4). For both cyanobacterial strains, differences between the number of proteins identified from biofilms formed

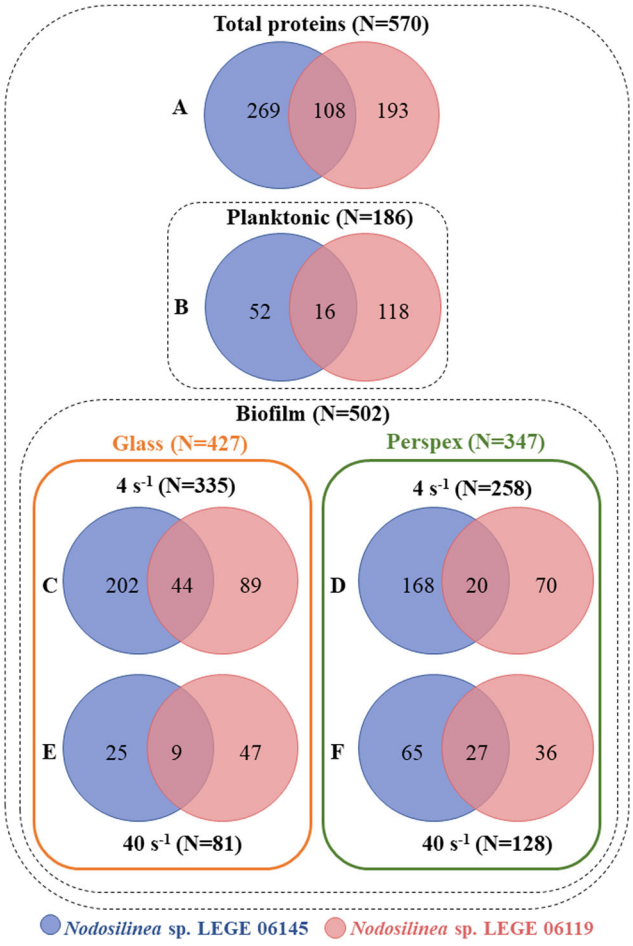

Figure 5. Venn diagrams obtained from the distribution of proteins identified among different conditions for the two cyanobacterial strains. The total of proteins for each condition is represented by (N=). The composite figure shows the unique and common proteins identified in both cyanobacterial strains at each condition represented from each Venn diagram: (A) total proteins identified on *Nodosilinea* sp. LEGE 06145 cells *vs* proteins identified on *Nodosilinea* sp. LEGE 06119 cells; (B) proteins identified on planktonic *Nodosilinea* sp. LEGE 06145 cells *vs* proteins identified on planktonic *Nodosilinea* sp. LEGE 06119 cells; (C) proteins identified on *Nodosilinea* sp. LEGE 06145 cells *vs* proteins identified on *Nodosilinea* sp. LEGE 06119 cells derived from biofilms formed on glass at $4\,s^{-1}$; (D) proteins identified on *Nodosilinea* sp. LEGE 06145 cells *vs* proteins identified on *Nodosilinea* sp. LEGE 06119 cells derived from biofilms formed on perspex at $4\,s^{-1}$; (E) proteins identified on *Nodosilinea* sp. LEGE 06145 cells *vs* proteins identified on *Nodosilinea* sp. LEGE 06119 cells derived from biofilms formed on glass at $40\,s^{-1}$; (F) proteins identified on *Nodosilinea* sp. LEGE 06145 cells *vs* proteins identified on *Nodosilinea* sp. LEGE 06119 cells derived from biofilms formed on perspex at $40\,s^{-1}$.

under different hydrodynamic conditions were more noticeable than those obtained for different surfaces (77.8% and 48.5% higher at $4\,s^{-1}$ than $40\,s^{-1}$ for *Nodosilinea* sp. LEGE 06145 and *Nodosilinea* sp. LEGE 06119, 28.1% and 33.4% higher on glass than perspex, for *Nodosilinea* sp. LEGE 06145 and *Nodosilinea* sp. LEGE 06119, respectively (Supplementary material, SM4). Except for the biofilms on glass at $40\,s^{-1}$ in which the number of proteins found in *Nodosilinea* sp. LEGE 06119 was 41.2% higher compared with *Nodosilinea* sp. LEGE 06145, in all biofilm samples, a higher number of proteins were identified in *Nodosilinea* sp. LEGE 06145. The complete list of identified proteins and their frequencies in different biofilm conditions is available in Supplementary material, SM5.

The identification and description of common proteins obtained from biofilm samples and for both cyanobacterial strains are presented in Table 1. While from biofilms formed on glass only one protein was identified in both cyanobacterial strains, 10 common proteins were identified from biofilms on the perspex surface. Additionally, 12 and 10 proteins for both cyanobacterial strains were identified in biofilm samples formed at $4\,s^{-1}$ and $40\,s^{-1}$, respectively. It should be noted that despite biofilm development being substantially lower in *Nodosilinea* sp. LEGE 06119 than *Nodosilinea* sp. LEGE 06145 (Supplementary material, SM2), these proteins were also found in this strain. The 50S ribosomal protein L7/L12 was identified in all biofilm conditions of the two cyanobacterial strains. This protein forms part of the ribosomal stalk, which helps the ribosome interact with guanosine triphosphate (GTP)-bound translation factors and it is responsible for accurate translation (Diaconu et al. 2005). This is an essential protein in the core metabolic functions and it was identified in all biofilm samples (Table 1 and Supplementary material, SM5). This result demonstrates the relevance and validity of the proteomic analysis performed in the present work. Additional cyanobacterial proteomic studies have revealed that 50% of proteins found could be assigned to core metabolic and transport functions (Anderson et al. 2006). However, a proteomic study performed with *Halorubrum lacusprofundi*, an extreme halophile archaeon, showed a decrease in the proteins involved in protein synthesis and folding in biofilms when compared with planktonic cells, including a large number of ribosomal proteins (Liao et al. 2016).

Proteins related to photosystems I and II and with allophycocyanin were found in three of the four biofilm condition groups (Table 1 in dark grey shading). The specific conditions in which these proteins were identified can be found in the Supplementary material, SM5. Photosystem I (PS I, plastocyaninferredoxin oxidoreductase) and photosystem II (PS II,

Table 1. Enumeration of proteins obtained from different biofilm samples in both cyanobacterial strains.

Biofilm development condition	Number of proteins found on both cyanobacterial strains	Accession number	Description
Glass	1	A0A1Z3HSI0	50S ribosomal protein L7/L12
Perspex	10	A0A077JIC2	Elongation factor Tu
		A0A0N7LBT2	Alkyl hydroperoxide reductase/thiol specific antioxidant/Mal allergen
		A0A1U7J348	Photosystem II CP43 reaction center protein
		A0A1U7J7J4	Allophycocyanin subunit beta
		A0A1U7JAP1	Allophycocyanin subunit beta
		A0A1U7JAR5	Photosystem I reaction center subunit X
		A0A1U7JAT3	Allophycocyanin
		A0A1Z3HSI0	50S ribosomal protein L7/L12
		A0A2P8ZU54	Photosystem I P700 chlorophyll a apoprotein A2
		I4HUB3	Carbon dioxide-concentrating mechanism protein CcmK
$4\,s^{-1}$	12	A0A073CH81	Photosystem I reaction center subunit XI
		A0A0N7LBT2	Alkyl hydroperoxide reductase/thiol specific antioxidant/Mal allergen
		A0A120MWU4	Transketolase
		A0A1U7J348	Photosystem II CP43 reaction center protein
		A0A1U7J7J4	Allophycocyanin subunit beta
		A0A1U7J8S7	Photosystem I reaction center subunit II
		A0A1Z3HSI0	50S ribosomal protein L7/L12
		A0A2P8VVE3	Allophycocyanin subunit beta
		A0A2P8W6V3	Amino acid ABC transporter substrate-binding protein
		A0A2P8ZWG1	HU family DNA-binding protein
		A0A2P8ZXU5	Phycobilisome rod-core linker polypeptide CpcG
		I4HUB3	Carbon dioxide-concentrating mechanism protein CcmK
$40\,s^{-1}$	7	A0A073CM30	PsaF
		A0A0U1Z975	Phycocyanin beta chain (Fragment)
		A0A1U7JAP1	Allophycocyanin subunit beta
		A0A1U7JAT3	Allophycocyanin
		A0A1Z3HSI0	50S ribosomal protein L7/L12
		A0A2P8ZU54	Photosystem I P700 chlorophyll a apoprotein A2
		K9F192	Phycobilisome protein

Note: For each protein, the frequency of appearance among the four biofilm conditions (glass, Perspex, $4\,s^{-1}$ and $40\,s^{-1}$) is indicated by different shaded colors (black – appearance in all four conditions; dark grey – appearance in three of four conditions; light grey – appearance in two of four conditions; without shading – appearance in only one of the four conditions).

waterplastoquinone oxidoreductase) are multisubunit protein complexes located in the thylakoid membranes of cyanobacteria, algae and higher plants (Nelson and Yocum 2006). Although in the present study the PsaF protein was only identified in biofilms of both the cyanobacterial strains formed at $40\,s^{-1}$ (Table 1), this protein is also related to photosystems (Photosystem I subunit III). A study performed by Huang et al. (2002) also identified proteins related to photosystems in the plasma membrane of *Synechocystis* PCC 6803. A proteomic study with different strains of *M. aeruginosa* showed that the majority of proteins shared among all strains were involved in photosynthesis and respiration (Alexova et al. 2011). Thus, the distribution of protein identification obtained in the present study is typical for cyanobacteria.

Allophycocyanin is a protein from the light-harvesting phycobiliprotein family, along with phycocyanin, phycoerythrin and phycoerythrocyanin, which may be found in the phycobilisome core complex (Sonani et al. 2015). Although proteins related to allophycocyanin were found in three of the four biofilm conditions, a protein fragment of phycocyanin beta chain and an additional non-specific phycobilisome protein were identified in both cyanobacterial strains for biofilms formed at $40\,s^{-1}$. Phycobilisomes are present in cyanobacteria and red algae and are formed by phycobiliproteins and also linker proteins (MacColl 1998). Allophycocyanin is considered an accessory pigment to chlorophyll and exhibits unique absorbance and fluorescence characteristics due to a lack of susceptibility to internal and external fluorescence quenching. Due to these features, allophycocyanin is ideal for highly sensitive studies such as flow cytometry and immunoassays (Manirafasha et al. 2016). Indeed, phycobiliproteins are regularly found in high abundance and they may constitute up to 50% of the total cellular protein of a cyanobacterium (Anderson et al. 2006). Previous proteomic studies with other cyanobacterial strains (*Synechocystis* PCC 6803) also identified proteins related to this phycobiliprotein family in their plasma membrane (Huang et al. 2002; Pisareva et al. 2007). In another study, which aimed to evaluate proteomic changes after heat

shock in *Synechocystis* PCC 6803, a decreased expression level for phycobilisome was observed (Slabas et al. 2006).

For both cyanobacterial strains, in biofilms formed on perspex and also at $4\,s^{-1}$ a protein from the peroxiredoxin superfamily was identified (alkyl hydroperoxide reductase/thiol specific antioxidant/Mal allergen). This protein protects cells against membrane oxidation through glutathione (GSH)-dependent reduction of phospholipid hydroperoxides to corresponding alcohols (Wood et al. 2003). A study performed with *Spirulina platensis*, which focused on comparative proteome analyses at low- and high-temperature stresses, indicated that low-temperature stress is tightly linked to oxidative stress as well as photosynthesis (Kurdrid et al. 2011). A quantitative proteomic study to define pathways and cellular processes involved in forming biofilms of *H. lacusprofundi* showed that these proteins associated with responses to oxidative stress are also related to biofilm forming ability (Liao et al. 2016). Although in the present study this protein was only found on perspex and also at $4\,s^{-1}$, this hydrodynamic condition resulted in greater biofilm development, which may have facilitated its detection.

Moreover, for both cyanobacterial strains, in biofilms formed on perspex and at $4\,s^{-1}$ a protein involved in the formation of the carboxysome (carbon dioxide-concentrating mechanism protein CcmK) was also found. Carboxysomes are polyhedral inclusion where the ribulose-1,5-bisphosphate carboxylase/oxygenase (Rubisco; the central enzyme in photosynthetic carbon assimilation) is sequestered. The CO_2 concentrating mechanism (CCM) is an adaptive and effective strategy evolved in cyanobacteria and also in eukaryotic microalgae for carbon acquisition, and it enables these organisms to survive when the CO_2 concentration limits photosynthesis (Wang et al. 2015). Baba et al. (2011) also studied this mechanism in the unicellular green alga *Chlamydomonas reinhardtii*. When the CO_2 concentration was elevated from the ambient air level to 3%, the algal growth rate increased 1.5-fold, and the amount and the composition of extracellular proteins clearly changed. However, significant changes were not found in intracellular proteins (Baba et al. 2011). In a study performed by Slabas et al. (2006), a decrease in Rubisco proteins was observed after heat shock in *Synechocystis* PCC 6803. Moreover, the CCM is a fundamental aspect of photosynthesis, metabolism, growth and biomass production in photosynthetic organisms and understanding this process provides guidance for potential molecular manipulation to improve biomass yield for commercial applications (Badger and Price 2003).

Despite the fact that in the present study, the elongation factor Tu and the amino acid ABC transporter substrate-binding protein were only identified for both cyanobacterial strains on biofilms formed on perspex and at $4\,s^{-1}$, respectively (Table 1), these proteins were found in other cyanobacterial studies, such as in the plasma membrane of *Synechocystis* PCC 6803 (Huang et al. 2002). Moreover, a higher abundance of elongation factors and ABC transporters in *Enterococcus faecalis* (Qayyum et al. 2016) and *H. lacusprofundi* (Liao et al. 2016) biofilms, respectively, was observed when compared with those obtained in planktonic cells.

Concluding remarks

In this study, standard methodologies for following cyanobacterial biofilm development were complemented with a qualitative proteomics approach. The results showed greater biofilm development at a lower shear rate ($4\,s^{-1}$) and it was also shown that hydrodynamic effects may be more important than surface properties in the formation of cyanobacterial biofilms. Moreover, the analysis of cyanobacterial biofilms by OCT is a useful methodology for understanding biofilm structure and dynamics under different conditions.

Cyanobacterial proteome analysis revealed that the strains under study had highly variable protein expression profiles, which may be a result of the adaptation of these organisms to the specific environmental niche that they occupy. Although this proteomic analysis was performed using a widely employed methodology and the proteome reported was biased on proteins expressed at higher levels, it is well known that there are limitations in the present technology for resolution and identification of proteins. Since none of the proteins identified in planktonic samples were exclusive to this form, that is, they were identified in an additional biofilm condition, the majority of the proteins were detected in both physiological states. The qualitative proteomic analysis investigated in this work was extremely relevant, given the few studies performed in this research field on filamentous cyanobacteria. Analyses of protein expression could provide an essential understanding of how cyanobacteria adapt to different environmental settings. However, in addition to studying which proteins were synthesized in the different conditions, it would be crucial to study the expression level of these

proteins, since biofilm development in these different conditions may be associated with quantitative differences in their proteome. Therefore, future work should focus on quantitative proteomic studies in order to allow the establishment of a relationship between the relative expression level of the identified proteins under different conditions. Moreover, due to their particular characteristics, cyanobacteria are promising organisms to be used in biotechnological processes. Vitamins, amino acids, fatty acids, lipopeptides and pigments belong to a broad spectrum of secondary metabolites and added-value compounds produced by cyanobacterial strains (Lau et al. 2015). For example, the allophycocyanin identified in two biofilm conditions of the present work is a valuable molecule to be applied in several biotechnological applications as fluorescent probes in flow cytometry and microarray assays, but also in the cosmetic, feed and food industries (Manirafasha et al. 2016). Moreover, as phycobiliproteins have been associated with antioxidant, anticancer and anti-inflammatory capacities, these compounds can also be used for medical purposes (Pagels et al. 2019). Improvements in cyanobacterial molecular biology are urgently required, since the omics tools available for these organisms are limited compared with heterotrophic model organisms (Sun et al. 2018).

Acknowledgements

This work was financially supported by: Base Funding - UIDB/00511/2020 of the Laboratory for Process Engineering, Environment, Biotechnology and Energy – LEPABE, funded by national funds through the FCT/MCTES (PIDDAC) and by the CVMAR+i – Industrial Innovation and Marine Biotechnology Valorisation, funded by INTERREG V A Espanha Portugal (POCTEP) [0302_CVMAR_I_1_P] and strategic funding UIDB/04423/2020 and UIDP/04423/2020 through national funds provided by FCT and European Regional Development Fund (ERDF), in the framework of the programme PT2020. M.J.R. acknowledges a PhD grant from FCT (SFRH/BD/140080/2018).

Disclosure statement

The authors declare that they have no conflict of interest.

ORCID

Maria João Leal Romeu http://orcid.org/0000-0002-1094-5425
Dany Domínguez-Pérez http://orcid.org/0000-0002-5211-972X
Daniela Almeida http://orcid.org/0000-0002-9874-933X
João Morais http://orcid.org/0000-0002-4190-0959
Alexandre Campos http://orcid.org/0000-0003-4621-885X
Vítor Vasconcelos http://orcid.org/0000-0003-3585-2417
Filipe J. M. Mergulhão http://orcid.org/0000-0001-5233-1037

References

Alexova R, Haynes PA, Ferrari BC, Neilan BA. 2011. Comparative protein expression in different strains of the bloom-forming cyanobacterium *Microcystis aeruginosa*. Mol Cell Proteom. 10:M110.003749. doi:10.1074/mcp.M110.003749

Allen AA, Habimana O, Casey E. 2018. The effects of extrinsic factors on the structural and mechanical properties of *Pseudomonas fluorescens* biofilms: a combined study of nutrient concentrations and shear conditions. Colloids Surf B Biointerf. 165:127–134. doi:10.1016/j.colsurfb.2018.02.035

Anderson DC, Campbell EL, Meeks JC. 2006. A soluble 3D LC/MS/MS proteome of the filamentous cyanobacterium *Nostoc punctiforme*. J Proteome Res. 5:3096–3104. doi:10.1021/pr060272m

Baba M, Suzuki I, Shiraiwa Y. 2011. Proteomic analysis of high-CO(2)-inducible extracellular proteins in the unicellular green alga, *Chlamydomonas reinhardtii*. Plant Cell Physiol. 52:1302–1314. doi:10.1093/pcp/pcr078

Babele PK, Kumar J, Chaturvedi V. 2019. Proteomic deregulation in cyanobacteria in response to abiotic stresses. Front Microbiol. 10:1–22. doi:10.3389/fmicb.2019.01315

Badger MR, Price GD. 2003. CO_2 concentrating mechanisms in cyanobacteria: molecular components, their diversity and evolution. J Exp Bot. 54:609–622. doi:10.1093/jxb/erg076

Bakke R, Kommedal R, Kalvenes S. 2001. Quantification of biofilm accumulation by an optical approach. J Microbiol Methods. 44:13–26. doi:10.1016/S0167-7012(00)00236-0

Battchikova N, Muth-Pawlak D, Aro EM. 2018. Proteomics of cyanobacteria: current horizons. Curr Opin Biotechnol. 54:65–71. doi:10.1016/j.copbio.2018.02.012

Bharti A, Velmourougane K, Prasanna R. 2017. Phototrophic biofilms: diversity, ecology and applications. J Appl Phycol. 29:2729–2744. doi:10.1007/s10811-017-1172-9

Campos A, Danielsson G, Farinha AP, Kuruvilla J, Warholm P, Cristobal S. 2016. Shotgun proteomics to unravel marine mussel (*Mytilus edulis*) response to long-term exposure to low salinity and propranolol in a Baltic Sea microcosm. J Proteomics. 137:97–106. doi:10.1016/j.jprot.2016.01.010

Canny J. 1986. A computational approach to edge detection. IEEE Trans Pattern Anal Mach Intell. 8:679–698. doi: 10.1109/TPAMI.1986.4767851.

Carvalho C. 2018. Marine biofilms: a successful microbial strategy with economic implications. Front Mar Sci. 5:1–11. doi:10.3389/fmars.2018.00126

Chen M, Hernandez-Prieto MA, Loughlin PC, Li Y, Willows RD. 2019. Genome and proteome of the chlorophyll f-producing cyanobacterium *Halomicronema hongdechloris*: adaptative proteomic shifts under different

light conditions. BMC Genomics. 20:1–15. doi:10.1186/s12864-019-5587-3
Crawford RJ, Webb HK, Truong VK, Hasan J, Ivanova EP. 2012. Surface topographical factors influencing bacterial attachment. Adv Colloid Interface Sci. 179–182:142–149. doi:10.1016/j.cis.2012.06.015
Delauney L, Compère C, Lehaitre M. 2010. Biofouling protection for marine environmental sensors. Ocean Sci. 6: 503–511. doi:10.5194/os-6-503-2010
Diaconu M, Kothe U, Schlünzen F, Fischer N, Harms JM, Tonevitsky AG, Stark H, Rodnina MV, Wahl MC. 2005. Structural basis for the function of the ribosomal L7/12 stalk in factor binding and GTpase activation. Cell. 121: 991–1004. doi:10.1016/j.cell.2005.04.015
Duda RO, Hart PE. 1972. Use of the Hough transformation to detect lines and curves in pictures. Commun Acm. 15: 11–15. doi:10.1145/361237
Faria SI, Teixeira-Santos R, Romeu MJ, Morais J, Vasconcelos V, Mergulhão FJ. 2020. The relative importance of shear forces and surface hydrophobicity on biofilm formation by coccoid cyanobacteria. Polymers (Basel). 12:653. doi:10.3390/polym12030653
Favre L, Ortalo-Magné A, Pichereaux C, Gargaros A, Burlet-Schiltz O, Cotelle V, Culioli G. 2018. Metabolome and proteome changes between biofilm and planktonic phenotypes of the marine bacterium *Pseudoalteromonas lipolytica* TC8. Biofouling. 34:132–148. doi:10.1080/08927014.2017.1413551
Flemming H-C, Murthy PS, Venkatesan R, Cooksey K. 2009. Marine and industrial biofouling. Costerton JW, editor. Los Angeles: Springer Berlin Heidelberg.
Heidari F, Hauer T, Zima J, Riahi H. 2018. New simple trichal cyanobacterial taxa isolated from radioactive thermal springs. Fottea. 18:137–149. doi:10.5507/fot.2017.024
Herschend J, Damholt ZBV, Marquard AM, Svensson B, Sørensen SJ, Hägglund P, Burmølle M. 2017. A metaproteomics approach to study the interspecies interactions affecting microbial biofilm development in a model community. Sci Rep. 7:1–13. doi:10.1038/s41598-017-16633-6
Huang F, Parmryd I, Nilsson F, Persson AL, Pakrasi HB, Andersson B, Norling B. 2002. Proteomics of *Synechocystis* sp. strain PCC 6803: identification of plasma membrane proteins. Mol Cell Proteom. 1: 956–966. doi:10.1074/mcp.m200043-mcp200
Jahn M, Vialas V, Karlsen J, Maddalo G, Edfors F, Forsström B, Uhlén M, Käll L, Hudson EP. 2018. Growth of cyanobacteria is constrained by the abundance of light and carbon assimilation proteins. Cell Rep. 25: 478–486.e8. doi:10.1016/j.celrep.2018.09.040
King RK, Flick GJ, Smith SA, Pierson MD, Boardman GD, Coale CW. 2006. Comparison of bacterial presence in biofilms on different materials commonly found in recirculating aquaculture systems. J Appl Aquac. 18:79–88. doi:10.1300/J028v18n01_05
Kotai J. 1972. Instructions for the preparation of modified nutrient solution Z8 for algae. Blindern, Oslo: Norwegian Institute for Water Research; vol. 11, p. 5.
Kurdrid P, Senachak J, Sirijuntarut M, Yutthanasirikul R, Phuengcharoen P, Jeamton W, Roytrakul S, Cheevadhanarak S, Hongsthong A. 2011. Comparative analysis of the *Spirulina platensis* subcellular proteome in response to low- and high-temperature stresses: uncovering cross-talk of signaling components. Proteome Sci. 9: 39. doi:10.1186/1477-5956-9-39
Lau NS, Matsui M, Abdullah AA. 2015. Cyanobacteria: photoautotrophic microbial factories for the sustainable synthesis of industrial products. Biomed Res Int. 2015: 754934. doi:10.1155/2015/754934
Leary DH, Li RW, Hamdan LJ, Hervey WJ, Lebedev N, Wang Z, Deschamps JR, Kusterbeck AW, Vora GJ. 2014. Integrated metagenomic and metaproteomic analyses of marine biofilm communities. Biofouling. 30:1211–1223. doi:10.1080/08927014.2014.977267
Liao Y, Williams TJ, Ye J, Charlesworth J, Burns BP, Poljak A, Raftery MJ, Cavicchioli R. 2016. Morphological and proteomic analysis of biofilms from the Antarctic archaeon. Sci Rep. 6:37454. doi:10.1038/srep3745
Lv J, Li N, Niu DK. 2008. Association between the availability of environmental resources and the atomic composition of organismal proteomes: evidence from *Prochlorococcus* strains living at different depths. Biochem Biophys Res Commun. 375:241–246. doi:10.1016/j.bbrc.2008.08.011
MacColl R. 1998. Cyanobacterial phycobilisomes. J Struct Biol. 124:311–334. doi:10.1006/jsbi.1998.4062
Manirafasha E, Ndikubwimana T, Zeng X, Lu Y, Jing K. 2016. Phycobiliprotein: potential microalgae derived pharmaceutical and biological reagent. Biochem Eng J. 109:282–296. doi:10.1016/j.bej.2016.01.025
Mayer MA, Borsdorf A, Wagner M, Hornegger J, Mardin CY, Tornow RP. 2012. Wavelet denoising of multiframe optical coherence tomography data. Biomed Opt Express. 3:572–589. doi:10.1364/BOE.3.000572
Mieszkin S, Callow ME, Callow JA. 2013. Interactions between microbial biofilms and marine fouling algae: a mini review. Biofouling. 29:1097–1113. doi:10.1080/08927014.2013.828712
Moreira JMR, Gomes LC, Simões M, Melo LF, Mergulhão FJ. 2015. The impact of material properties, nutrient load and shear stress on biofouling in food industries. Food Bioprod Process. 95:228–236. doi:10.1016/j.fbp.2015.05.011
Muthusamy S, Lundin D, Mamede Branca RM, Baltar F, González JM, Lehtiö J, Pinhassi J. 2017. Comparative proteomics reveals signature metabolisms of exponentially growing and stationary phase marine bacteria. Environ Microbiol. 19:2301–2319. doi:10.1111/1462-2920.13725
Nelson N, Yocum CF. 2006. Structure and function of photosystems I and II. Annu Rev Plant Biol. 57:521–565. doi:10.1146/annurev.arplant.57.032905.105350
Otsuka S, Suda S, Shibata S, Oyaizu H, Matsumoto S, Watanabe MM. 2001. A proposal for the unification of five species of the cyanobacterial genus *Microcystis* Kützing ex Lemmermann 1907 under the rules of the Bacteriological Code. Int J Syst Evol Microbiol. 51: 873–879. doi:10.1099/00207713-51-3-873
Ow SY, Salim M, Noirel J, Evans C, Wright PC. 2011. Minimising iTRAQ ratio compression through understanding LC-MS elution dependence and high-resolution HILIC fractionation. Proteomics. 11:2341–2346. doi:10.1002/pmic.201000752

Pagels F, Guedes AC, Amaro HM, Kijjoa A, Vasconcelos V. 2019. Phycobiliproteins from cyanobacteria: chemistry and biotechnological applications. Biotechnol Adv. 37: 422–443. doi:10.1016/j.biotechadv.2019.02.010

Pandhal J, Ow SY, Wright PC, Biggs CA. 2009. Comparative proteomics study of salt tolerance between a nonsequenced extremely halotolerant cyanobacterium and its mildly halotolerant relative using in vivo metabolic labeling and in vitro isobaric labeling. J Proteome Res. 8:818–828. doi:10.1021/pr800283q

Parnasa R, Nagar E, Sendersky E, Reich Z, Simkovsky R, Golden S, Schwarz R. 2016. Small secreted proteins enable biofilm development in the cyanobacterium *Synechococcus elongatus*. Sci Rep. 6:32209. doi:10.1038/srep32209

Perkerson Iii RB, Johansen JR, Kováčik L, Brand J, Kaštovský J, Casamatta DA. 2011. A unique pseudanabaenalean (Cyanobacteria) genus *Nodosilinea* gen. nov. based on morphological and molecular DATA(1). J Phycol. 47:1397–1412. doi:10.1111/j.1529-8817.2011.01077.x

Pisareva T, Shumskaya M, Maddalo G, Ilag L, Norling B. 2007. Proteomics of *Synechocystis* sp. PCC 6803. Identification of novel integral plasma membrane proteins. Febs J. 274:791–804. doi:10.1111/j.1742-4658.2006.05624.x

Porra R, Thompson W, Kriedemann P. 1989. Determination of accurate extinction coefficients and simultaneous equations for assaying chlorophylls *a* and *b* extracted with four different solvents: verification of the concentration of chlorophyll standards by atomic absorption spectroscopy. Biochim Biophys Acta. 975:384–394. doi:10.1016/S0005-2728(89)80347-0

Qayyum S, Sharma D, Bisht D, Khan AU. 2016. Protein translation machinery holds a key for transition of planktonic cells to biofilm state in *Enterococcus faecalis*: a proteomic approach. Biochem Biophys Res Commun. 474:652–659. doi:10.1016/j.bbrc.2016.04.145

Radzi R, Muangmai N, Broady P, Wan Omar WM, Lavoue S, Convey P, Merican F. 2019. *Nodosilinea signiensis* sp. nov. (Leptolyngbyaceae, Synechococcales), a new terrestrial cyanobacterium isolated from mats collected on Signy Island, South Orkney Islands, Antarctica. PLoS One. 14:e0224395. doi:10.1371/journal.pone.0224395

Ramos V, Morais J, Castelo-Branco R, Pinheiro Â, Martins J, Regueiras A, Pereira AL, Lopes VR, Frazão B, Gomes D, et al. 2018. Cyanobacterial diversity held in microbial biological resource centers as a biotechnological asset: the case study of the newly established LEGE culture collection. J Appl Phycol. 30:1437–1451. doi:10.1007/s10811-017-1369-y

Romeu MJ, Alves P, Morais J, Miranda JM, de Jong ED, Sjollema J, Ramos V, Vasconcelos V, Mergulhão F. 2019. Biofilm formation behaviour of marine filamentous cyanobacterial strains in controlled hydrodynamic conditions. Environ Microbiol. 21:4411–4424. doi:10.1111/1462-2920.14807

Slabas AR, Suzuki I, Murata N, Simon WJ, Hall JJ. 2006. Proteomic analysis of the heat shock response in *Synechocystis* PCC6803 and a thermally tolerant knockout strain lacking the histidine kinase 34 gene. Proteomics. 6:845–864. doi:10.1002/pmic.200500196

Sonani RR, Gupta GD, Madamwar D, Kumar V. 2015. Crystal structure of allophycocyanin from marine cyanobacterium *Phormidium* sp. Plos One. 10:e0124580. doi:10.1371/journal.pone.0124580

Sun T, Li S, Song X, Diao J, Chen L, Zhang W. 2018. Toolboxes for cyanobacteria: recent advances and future direction. Biotechnol Adv. 36:1293–1307. doi:10.1016/j.biotechadv.2018.04.007

Taylor DA. 1996. Introduction to marine engineering. Burlington, MA: Butterworth-Heinemann.

Telegdi J, Trif L, Románszki L. 2016. Smart anti-biofouling composite coatings for naval applications. In: Montemor MF, editor. Smart composite coatings and membranes transport, structural, environmental and energy applications. Cambridge, UK: Woodhead Publishing; p. 123–155.

Teodósio JS, Simões M, Melo LF, Mergulhão FJ. 2011. Flow cell hydrodynamics and their effects on *E. coli* biofilm formation under different nutrient conditions and turbulent flow. Biofouling. 27:1–11. doi:10.1080/08927014.2010.535206

Vázquez-Martínez J, Gutierrez-Villagomez JM, Fonseca-García C, Ramírez-Chávez E, Mondragón-Sánchez ML, Partida-Martínez L, Johansen JR, Molina-Torres J. 2018. *Nodosilinea chupicuarensis* sp. nov. (Leptolyngbyaceae, Synechococcales) a subaerial cyanobacterium isolated from a stone monument in central Mexico. Phytotaxa. 334:167. doi:10.11646/phytotaxa.334.2.6

Wang N, Sadiq FA, Li S, He G, Yuan L. 2020. Tandem mass tag-based quantitative proteomics reveals the regulators in biofilm formation and biofilm control of *Bacillus licheniformis*. Food Control. 110:107029. doi:10.1016/j.foodcont.2019.107029

Wang Y, Stessman DJ, Spalding MH. 2015. The CO_2 concentrating mechanism and photosynthetic carbon assimilation in limiting CO2: how Chlamydomonas works against the gradient. Plant J. 82:429–448. doi:10.1111/tpj.12829

Wiśniewski JR, Zougman A, Nagaraj N, Mann M. 2009. Universal sample preparation method for proteome analysis. Nat Methods. 6:359–362. doi:10.1038/nmeth.1322

Wood ZA, Schröder E, Harris JR, Poole LB. 2003. Structure, mechanism and regulation of peroxiredoxins. Trends Biochem Sci. 28:32–40. doi:10.1016/S0968-0004(02)00003-8